ISSN: 2277-3754
ISO 9001:2008 Certified
International Journal of Engineering and Innovative Technology (IJEIT)
Volume 3, Issue 1, July 2013

Transient Thermo elastic Problem of a Circular Plate with Heat Generation

N. W. Khobragade[1] , L. H.Khalsa[2] , T. T. Gahane[3] and A. C. Pathak
1. Professor, Department of Mathematics, RTM Nagpur University, Nagpur, India.
2. Professor, Department of Mathematics, M.G. College, Armori, Gadchiroli, India
3,4 .Research Scholar, Department of Mathematics, RTM Nagpur University, Nagpur, India

Abstract - We apply integral transformation techniques to study thermoelastic response of a circular plate, in general in which sources are generated according to the linear function of the temperature, with boundary conditions of the radiation type. The results are obtained as series of Bessel functions. Numerical calculations are carried out for a particular case of a plate made of Aluminum metal and the results are depicted in figures.

Keywords: **Transient response, circular plate, temperature distribution, thermal stress, integral transform**

I. INTRODUCTION

Nowacki [5] has determined steady-state thermal stresses in a thick circular plate subjected to an axisymmetric temperature distribution on the upper face with zero temperature on the lower face circular edge. Wankhede [9] has determined the quasi-static thermal stresses in circular plate subjected to arbitrary initial temperature on the upper face with lower face at zero temperature. However there aren't many investigations on transient state. Roy Choudhuri [8] has succeeded in determined the quasi static thermal stresses in a circular place subjected to transient temperature along the circumference of circular upper face with lower face at zero temperature and the fixed circular edge thermally insulated. in a recent work, same problems have been solved by Noda et al. [6] and Deshmukh et al. [1]. In all aforementioned investigations an axisymmetrically heated plate has been considered.

Recently Nasser [3,4] proposed the concept of heat sources in generalized thermo elasticity and applied to a thick plate problem. They have not however considered any thermoelastic problem with boundary conditions of radiation type in which source are generated according to the linear function of the temperature, which satisfies the time dependent heat conduction equation. From the previous literature regarding circular solid cylinder as considered, it was observed by the author that no analytical procedure has been established considering internal heat source generation within the body. This Paper is concerned with the transient thermoelastic problem of a circular plate in which sources are generated according to the linear function of temperature occupying the space

$$D=\{(x,y,z)\in R^3 \ : \ 0\le (x^2+y^2)^{1/2}\le a, \quad -h\le z\le h\}$$

where $r=(x^2+y^2)^{1/2}$ with radiation type boundary conditions.

II. STATEMENT OF THE PROBLEM

Consider a circular plate in which sources are generated according to the linear function of temperature. The material is isotropic, homogeneous and all properties are assumed to be constant. Heat conduction with internal heat source and the prescribed boundary conditions of the radiation type is considered. The equation for heat conduction is given by

$$k\left[\frac{1}{r}\frac{\partial}{\partial r}\left(r\frac{\partial\theta}{\partial r}\right)+\frac{\partial^2\theta}{\partial z^2}\right]+\Theta(r,z,t,\theta)=\frac{\partial\theta}{\partial t} \qquad (1)$$

where $\Theta(r,z,t,\theta)$ is the source function and $k=\lambda/\rho C$ being the thermal conductivity of the material, ρ is the density and C is the calorific capacity, assumed to be constant. For convenience, we consider the under given functions as the superposition of the simpler function [2]

$$\Theta(r,z,t,\theta)=\Phi(r,z,t)+\Psi(t)\,\theta(r,z,t) \qquad (2)$$

and

$$T(r,z,t)=\theta(r,z,t)\exp\left[-\int_0^t\Psi(\zeta)d\zeta\right] \qquad (3)$$

$$\chi(r,z,t)=\Phi(r,z,t)\exp\left[-\int_0^t\Psi(\zeta)d\zeta\right]$$

or for the sake of brevity, we consider

$$\chi(r,z,t)=\frac{\delta(r-r_0)\delta(z-z_0)}{2\pi r_0}\exp(-\omega t),$$

$0\le r_0\le a, \quad -h\le z_0\le h, \quad \omega>0$.

Substituting equations (2) and (3) in the heat conduction equation (1), one obtains

$$k\left[\frac{1}{r}\frac{\partial}{\partial r}\left(r\frac{\partial T}{\partial r}\right)+\frac{\partial^2 T}{\partial z^2}\right]+\chi(r,z,t)=\frac{\partial T}{\partial t} \qquad (4)$$

where k is the thermal diffusivity of the material of the cylinder (which is assumed to be constant), subject to the initial and boundary conditions

$T(r,z,t)=f(r,z)$ at $t=0$ for all $0\le r\le a, \ -h\le z\le h$ (5)

$T(r,z,t)=0$ at $r=a$ for all $-h\le z\le h, \ t>0$

ISSN: 2277-3754
ISO 9001:2008 Certified
International Journal of Engineering and Innovative Technology (IJEIT)
Volume 3, Issue 1, July 2013

(6)

$$\left[T + k_1 \frac{\partial T}{\partial z}\right]_{z=h} = \exp(-\omega t)\delta(r - r_0) \quad \text{for all} \quad 0 \le r \le a,$$

$$t > 0. \qquad (7)$$

$$\left[T + k_2 \frac{\partial T}{\partial z}\right]_{z=-h} = \exp(-\omega t)\delta(r - r_0) \quad \text{for all} \quad 0 \le r \le a,$$

$$t > 0. \qquad (8)$$

where $\delta(r - r_0)$ is the Dirac Delta function having $0 \le r_0 \le a$, $\omega > 0$ is a constant; $\exp(-\omega t)\delta(r - r_0)$ is the additional sectional heat available on its surface at $z = -h, h$; k_1 and k_2 are radiation constants on the upper and lower surface of the cylinder respectively.

The Navier's equations without the body forces for axisymmetric two-dimensional thermoelastic problem can be expressed as [6]

$$\nabla^2 u_r - \frac{u_r}{r^2} + \frac{1}{1-2\nu}\frac{\partial e}{\partial r} - \frac{2(1+\nu)}{1-2\nu} a_t \frac{\partial \theta}{\partial r} = 0$$

$$\nabla^2 u_z - \frac{1}{1-2\nu}\frac{\partial e}{\partial z} - \frac{2(1+\nu)}{1-2\nu} a_t \frac{\partial \theta}{\partial z} = 0 \qquad (9)$$

where u_r and u_z are the displacement components in the radial and axial directions, respectively and the dilatation e as

$$e = \frac{\partial u_r}{\partial r} + \frac{u_r}{r} + \frac{\partial u_z}{\partial z}$$

The displacement function in the cylindrical coordinate system are represented by the Goodier's thermoelastic displacement potential $\phi(r, z, t)$ and Michell's function M as [**6**]

$$u_r = \frac{\partial \phi}{\partial r} - \frac{\partial^2 M}{\partial r \partial z} \qquad (10)$$

$$u_z = \frac{\partial \phi}{\partial z} + 2(1-\nu)\nabla^2 M - \frac{\partial^2 M}{\partial z^2} \qquad (11)$$

in which Goodier's thermoelastic potential must satisfy the equation

$$\nabla^2 \phi = \left(\frac{1+\nu}{1-\nu}\right) a_t \theta \qquad (12)$$

and the Michell's function M must satisfy the equation

$$\nabla^2 (\nabla^2 M) = 0 \qquad (13)$$

where $\nabla^2 = \frac{1}{r}\frac{\partial}{\partial r}\left(r\frac{\partial}{\partial r}\right) + \frac{\partial^2}{\partial z^2}$

The component of the stresses are represented by the use of potential ϕ and Michell's function M as

$$\sigma_{rr} = 2G\left\{\left(\frac{\partial^2 \phi}{\partial r^2} - \nabla^2 \phi\right) + \frac{\partial}{\partial z}\left(\nu \nabla^2 M - \frac{\partial^2 M}{\partial r^2}\right)\right\} \qquad (14)$$

$$\sigma_{\theta\theta} = 2G\left\{\left(\frac{1}{r}\frac{\partial \phi}{\partial r} - \nabla^2 \phi\right) + \frac{\partial}{\partial z}\left(\nu \nabla^2 M - \frac{1}{r}\frac{\partial M}{\partial r}\right)\right\} \qquad (15)$$

$$\sigma_{zz} = 2G\left\{\left(\frac{\partial^2 \phi}{\partial z^2} - \nabla^2 \phi\right) + \frac{\partial}{\partial z}\left((2-\nu)\nabla^2 M - \frac{\partial^2 M}{\partial z^2}\right)\right\} \qquad (16)$$

And

$$\sigma_{rz} = 2G\left\{\frac{\partial^2 \phi}{\partial r \partial z} + \frac{\partial}{\partial r}\left((1-\nu)\nabla^2 M - \frac{\partial^2 M}{\partial z^2}\right)\right\} \qquad (17)$$

where G and ν are the shear modulus and Poisson's ratio respectively.

The boundary conditions on the traction free surface of a solid cylinder are

$$\sigma_{rr} = \sigma_{rz} = 0 \text{ at } r = a \qquad (18)$$

The equations (2.1) to (2.18) constitute the mathematical formulation of the problem under consideration.

III. SOLUTION OF THE PROBLEM

Applying finite Hankel transform to the equation (4) and using boundary condition (6), we get

$$k\left(\frac{d^2 \bar{T}}{dz^2} - \mu_n^2 \bar{T}\right) + \bar{\chi} = \frac{d\bar{T}}{dt} \qquad (19)$$

where $\bar{T}$ is the Hankel transform of T and μ_n is the Hankel transform parameter.

Further, we apply finite Marchi-Fasulo transform to the equation (19) to get

$$\frac{d\bar{T}^*}{dt} + kp^2 \bar{T}^* = ke^{-\omega t}\left(\frac{P_m(h)}{k_1} - \frac{P_m(-h)}{k_2}\right) + \bar{\chi}^* \qquad (20)$$

where $\bar{T}^*$ is the finite Marchi-Fasulo transform of $\bar{T}$ and λ_m is the Marchi-Fasulo transform parameter,

$$P_m(z) = Q_m \cos(a_m z) - W_m \sin(a_m z)$$

$$Q_m = a_m(k_1 + k_2)\cos(a_m h)$$

$$W_m = 2\cos(a_m h) + (k_2 - k_1)a_m \sin(a_m h)$$

The Eigen values a_m are the positive roots of the characteristic equation

$$[k_1 a \cos(ah) + \sin(ah)][\cos(ah) + k_2 a \sin(ah)]$$

$$= [k_2 a \cos(ah) - \sin(ah)][\cos(ah) - k_1 a \sin(ah)]$$

ISSN: 2277-3754
ISO 9001:2008 Certified
International Journal of Engineering and Innovative Technology (IJEIT)
Volume 3, Issue 1, July 2013

The solution of differential equation (20) is given by

$$\bar{T}^*(\mu_n,\lambda_m,t) = e^{-kp^2t}[B(m)e^{-(\omega-kp^2)t} + 2kp^2\int \bar{\chi}^* e^{kp^2t}dt + \bar{f}^*] \quad (21)$$

where $B(m) = \dfrac{-k}{kp^2+w}\left(\dfrac{P_m(h)}{k_1} - \dfrac{P_m(-h)}{k_2}\right)$

Now, applying inversion of finite Marchi-Fasulo transform and Hankel transform to the equation (21) to get

$$T = \frac{2}{a^2}\sum_{m,n=1}^{\infty}\frac{J_0(r\xi_m)}{[J_0'(a\xi_n)]^2}\frac{P_m(z)}{\lambda_m}e^{-kp^2t} \times[B(m)e^{-(\omega-kp^2)t} + 2kp^2\int \bar{\chi}^* e^{kp^2t}dt + \bar{f}^*] \quad (22)$$

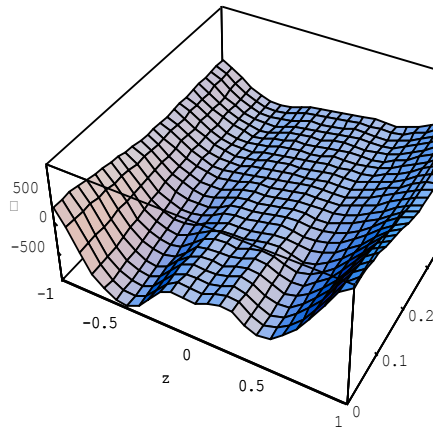

Fig 1: Temperature distribution along *r*- and *z*-direction for *t* =3

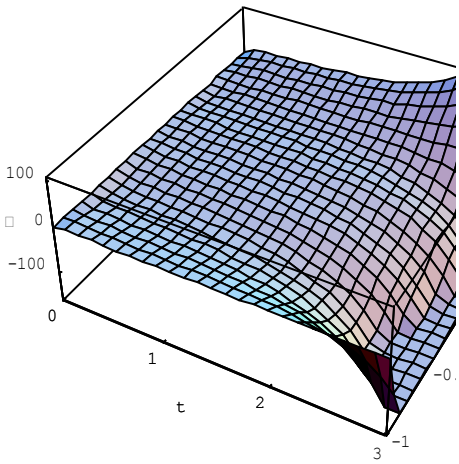

Fig 2: Temperature distribution along *z*-direction with varying time for r = 0.5

Fig. 1 shows the temperature distribution along the r and z direction of the circular plate at *t* = 3. It is observed that due to the width of the plate, increase in temperature was found at the beginning. Finally temperature distribution further increase and attains zero value at the extreme end. Fig. 2 and Fig 3 show the temperature distribution with varying time function along *z*-direction and *r*-direction and increased temperature trend is observed at *z* = 1 where we have provided additional sectional heat supply on its flat surface. As the time increases, the temperature distribution gradually increases from the center of core to the outer edge.

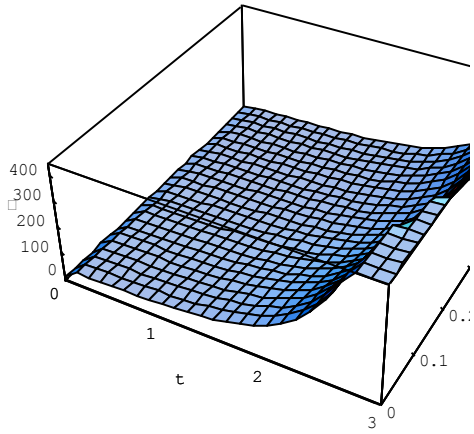

Fig 3: Temperature distribution along *r*-direction with varying time for z = 1.

The solution for the displacement function are represented by the Goodier's thermoelastic displacement potential ϕ governed by equation (11) is given by

$$\phi = \left(\frac{1+\nu}{1-\nu}\right)\frac{r^2a_t}{2a^2}\sum_{m,n=1}^{\infty}\frac{J_0(r\xi_m)}{[J_0'(a\xi_n)]^2}\frac{P_m(z)}{\lambda_m}e^{-kp^2t} \times[B(m)e^{-(\omega-kp^2)t} + 2kp^2\int \bar{\chi}^* e^{kp^2t}dt + \bar{f}^*] \quad (23)$$

The solution for Michell's function M are assumed so as to satisfy the governed condition of equation (12) as

$$M = \left(\frac{1+\nu}{1-\nu}\right)\frac{r^2a_t}{2a^2}\sum_{m,n=1}^{\infty}\frac{J_0(r\xi_m)}{[J_0'(a\xi_n)]^2}e^{-kp^2t} \times[A_nJ_0(\beta_nr) + C_n(\beta_nr)J_1(\beta_nr)]\cosh(\beta_nz) \times[B(m)e^{-(\omega-kp^2)t} + 2kp^2\int \bar{\chi}^* e^{kp^2t}dt + \bar{f}^*] \quad (24)$$

Using equations (22) and (23) in equations (9) and (10), the displacement components are obtained as

$$u_r = -\left(\frac{1+\nu}{1-\nu}\right)\frac{a_t}{2a^2}\sum_{m,n=1}^{\infty}\frac{\beta_n\sinh(\beta_nz)}{[J_0'(a\xi_n)]^2}e^{-kp^2t} \times[B(m)e^{-(\omega-kp^2)t} + 2kp^2\int \bar{\chi}^* e^{kp^2t}dt + \bar{f}^*] \times\Big\{ r^2J_0(r\xi_n)[A_nJ_0'(\beta_nr) + C_n(\beta_nr)J_1'(\beta_nr)] + C_n\beta_nJ_1(\beta_nr)] \times\left[A_nJ_0(\beta_nr) + C_n(\beta_nr)J_1(\beta_nr)] - \frac{P_m(z)}{\lambda_m\beta_n\sinh(\beta_nz)}\right] \times[r^2J_0'(r\xi_n) + 2rJ_0(r\xi_n)]\Big\} \quad (25)$$

ISSN: 2277-3754
ISO 9001:2008 Certified
International Journal of Engineering and Innovative Technology (IJEIT)
Volume 3, Issue 1, July 2013

$$u_z = \left(\frac{1+\nu}{1-\nu}\right)\frac{a_t}{2a^2}\sum_{m,n=1}^{\infty}\frac{\cosh(\beta_n z)}{[J_0'(a\xi_n)]^2}\; e^{-kp^2 t}$$
$$\times[B(m)e^{-(\omega-kp^2)t} + 2kp^2\int \bar{\chi}^* e^{kp^2 t}dt + \bar{f}^*]$$
$$\times\left\{\frac{r^2 J_0(r\xi_n)P_m'(z)}{\lambda_m \cosh(\beta_n z)} + 2r^2(1-\nu)J_0(r\xi_n)\right.$$
$$\times\left[A_n J_0''(\beta_n r)+C_n(\beta_n r)J_1''(\beta_n r)\right]+2C_n\beta_n J_1'(\beta_n r)\Big]$$
$$+[4r^2(1-\nu)J_0'(r\xi_n)+10r(1-\nu)J_0(r\xi_n)]$$
$$\times\left[A_n J_0'(\beta_n r)+C_n(\beta_n r)J_1'(\beta_n r)+C_n\beta_n J_1(\beta_n r)\right]$$
$$+[2r^2(1-\nu)J_0''(r\xi_n)+10r(1-\nu)J_0'(r\xi_n)$$
$$+(8-8\nu+\beta_n^2 r^2-2\nu\beta_n^2 r^2)J_0(r\xi_n)]$$
$$\left.\times[A_n J_0(\beta_n r)+C_n(\beta_n r)J_1(\beta_n r)]\right\} \quad (26)$$

The stress components can be calculated by substituting the values of thermoelastic displacement potential ϕ from equation (22) and Michel's function M from equation (23) in equations (13) to (16), one obtain the stress functions as

$$\sigma_{rr} = -2G\left(\frac{1+\nu}{1-\nu}\right)\frac{a_t}{2a^2}\sum_{m,n=1}^{\infty}\frac{\sinh(\beta_n z)}{[J_0'(a\xi_n)]^2}\; e^{-kp^2 t}$$
$$\times[B(m)e^{-(\omega-kp^2)t} + 2kp^2\int \bar{\chi}^* e^{kp^2 t}dt + \bar{f}^*]$$
$$\times\left\{\frac{1}{\lambda_m \sinh(\beta_n z)}[rP_m(z)J_0'(r\xi_n)+(2P_m(z)+r^2P_m''(z))J_0(r\xi_n)\right.$$
$$-\beta_n r^2(\nu-1)J_\mu(r\xi_n)\left[A_n J_0''(\beta_n r)+C_n(\beta_n r)J_1''(\beta_n r)\right]+2C_n\beta_n J_1'(\beta_n r)\Big]$$
$$-[2(\nu-1)\beta_n r^2 J_0(r\xi_n)+r\beta_n(5\nu-4)J_0(r\xi_n)]$$
$$\times\left[A_n J_0'(\beta_n r)+C_n(\beta_n r)J_1'(\beta_n r)\right]+C_n\beta_n J_1(\beta_n r)\Big]$$
$$-[(\nu-1)\beta_n r^2 J_0''(r\xi_n)+r\beta_n(5\nu-4)J_0'(r\xi_n)+\beta_n(\nu\beta_n^2 r^2+4\nu-2)J_0(r\xi_n)]$$
$$\left.\times[A_n J_0(\beta_n r)+C_n(\beta_n r)J_1(\beta_n r)]\right\} \quad (27)$$

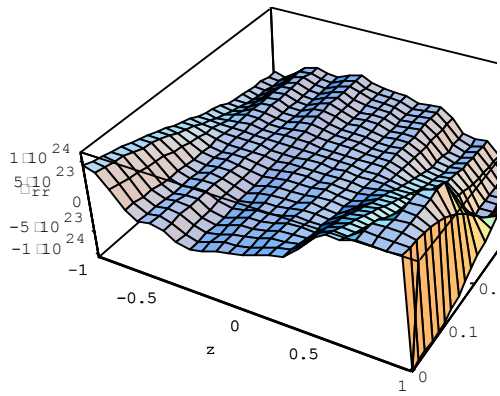

Fig. 4: Radial stress distribution along *r*- and *z*- direction for *t* =3

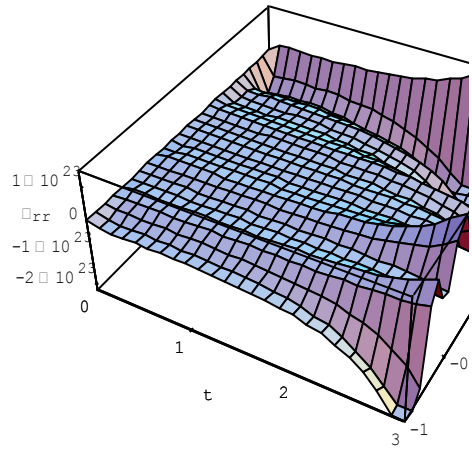

Fig 5: Radial stress distribution along *z*-direction with varying time for r = 0.5

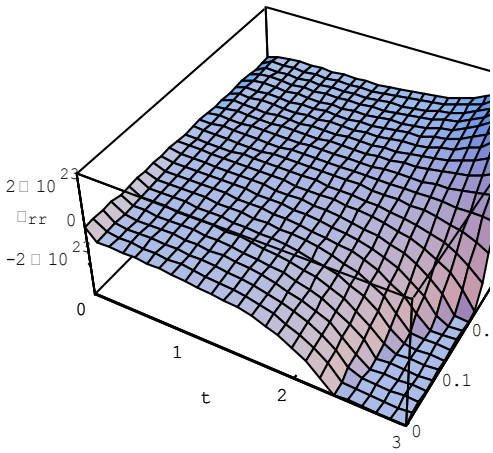

Fig. 6: Radial stress distribution along *r*-direction with varying time for z = 1.

Fig. 4 and Fig. 5 shows the radial stress distribution σ_{rr} along the r and z direction of the plate with varying time. From the figure, the location of points of minimum stress occurs at the end points, while the thermal stress response is maximum at the inner surface. Fig. 6 shows the radial stress distribution σ_{rr} along the radial direction of the plate with varying time. It is observed that stress at the outer extreme end is high and it gradually decreases towards the center core.

$$\sigma_{\theta\theta} = -2G\left(\frac{1+\nu}{1-\nu}\right)\frac{a_t}{2a^2}\sum_{m,n=1}^{\infty}\frac{\sinh(\beta_n z)}{[J_0'(a\xi_n)]^2}\; e^{-kp^2 t}$$
$$\times[B(m)e^{-(\omega-kp^2)t} + 2kp^2\int \bar{\chi}^* e^{kp^2 t}dt + \bar{f}^*]$$
$$\times\left\{\frac{P_m(z)}{\lambda_m \sinh(\beta_n z)}[r^2 J_0''(r\xi_n)+4rJ_0'(r\xi_n)+\left(\frac{r^2P_m''(z)+2P_m(z)}{P_m(z)}\right)J_0(r\xi_n)]\right.$$
$$-\nu\beta_n r^2 J_0(r\xi_n)\left[A_n J_0''(\beta_n r)+C_n(\beta_n r)J_1''(\beta_n r)\right]+2C_n\beta_n J_1'(\beta_n r)\Big]$$
$$-r\beta_n[2\nu r J_0'(r\xi_n)+(5\nu-1)J_0(r\xi_n)]$$
$$\times\left[A_n J_0'(\beta_n r)+C_n(\beta_n r)J_1'(\beta_n r)+C_n\beta_n J_1(\beta_n r)\right]$$

ISSN: 2277-3754
ISO 9001:2008 Certified
International Journal of Engineering and Innovative Technology (IJEIT)
Volume 3, Issue 1, July 2013

$$-\beta_n[\nu r^2 J_0''(r\xi_n)+r(5\nu-1)J_0'(r\xi_n)+(\nu\beta_n^2 r^2+4\nu-2)J_0(r\xi_n)]$$
$$\times[A_n J_0(\beta_n r)+C_n(\beta_n r)J_1(\beta_n r)]\Big\} \quad (28)$$

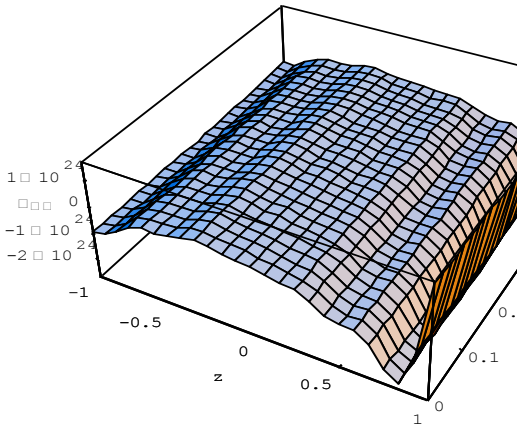

Fig. 7: Tangential stress distribution along *r*- and *z*-direction for *t* =3

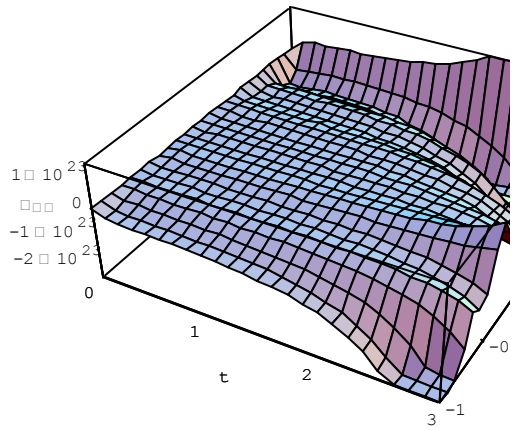

Fig. 8: Tangential stress distribution along *z*-direction with varying time for r = 0.5

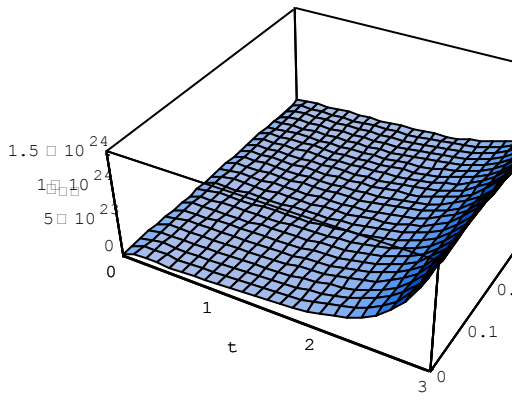

Fig. 9: Tangential stress distribution along *r*-direction with varying time for t =3

Fig. 7 shows the tangential stress distribution $\sigma_{\theta\theta}$ along the radial and thickness direction of the plate at *t* =3. Fig. 8 shows the stress distribution along *z*-direction with varying time. Fig. 9 shows the tangential stress distribution along the r- direction of the plate with varying time. It is observed that stress gradually increases with time.

$$\sigma_{zz}=-2G\left(\frac{1+\nu}{1-\nu}\right)\frac{a_t}{2a^2}\sum_{m,n=1}^{\infty}\frac{\beta_n\sinh(\beta_n z)}{[J_0'(a\xi_n)]^2}$$
$$\times[B(m)e^{-(\omega-kp^2)t}+2kp^2\int\bar{\chi}^*e^{kp^2t}dt+\bar{f}^*]$$
$$\times\left\{\frac{P_m(z)}{\lambda_m\sinh(\beta_n z)}[r^2J_0''(r\xi_n)+5rJ_0'(r\xi_n)+4J_0(r\xi_n)]\right.$$
$$-(2-\nu)r^2J_0(r\xi_n)[A_nJ_0''(\beta_n r)+C_n(\beta_n r)J_1''(\beta_n r)]+2C_n\beta_nJ_1'(\beta_n r)]$$
$$-(2-\nu)r[2rJ_0'(r\xi_n)+5J_0(r\xi_n)]$$
$$\times[A_nJ_0'(\beta_n r)+C_n(\beta_n r)J_1'(\beta_n r)+C_n\beta_nJ_1(\beta_n r)]$$
$$-[r^2(2-\nu)J_0''(r\xi_n)+5r(2-\nu)J_0'(r\xi_n)+(8-4\nu+\beta_n^2r^2-\nu\beta_n^2r^2)J_0(r\xi_n)]$$
$$\times[A_nJ_0(\beta_n r)+C_n(\beta_n r)J_1(\beta_n r)]\Big\} \quad (29)$$

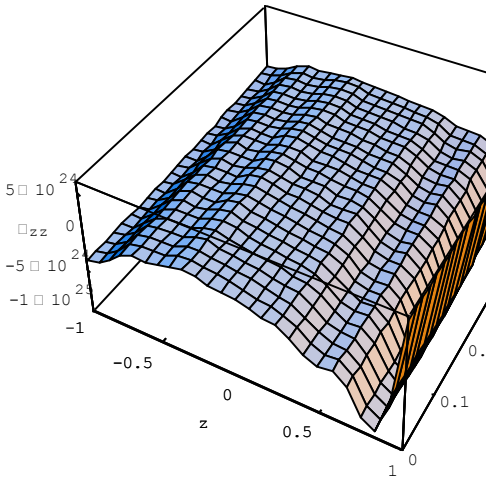

Fig. 10: Axial stress distribution along *r*- and *z*- direction for *t* =3

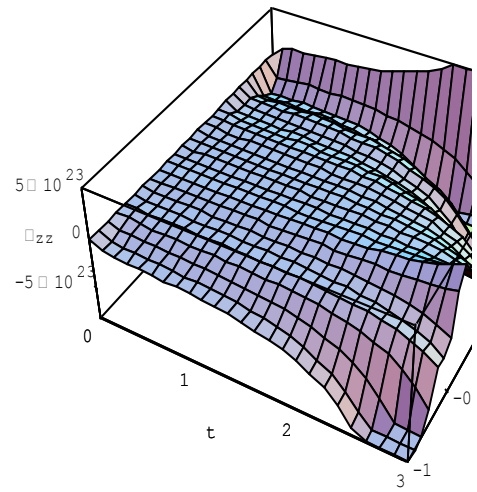

Fig. 11: Axial stress distribution along *z*-direction with varying time for r = 0.5

Fig. 10, Fig. 11 and Fig. 12 shows the axial stress distribution σ_{zz}, which is similar in nature, but higher in magnitude as compared to tangential stress component.

ISSN: 2277-3754
ISO 9001:2008 Certified
International Journal of Engineering and Innovative Technology (IJEIT)
Volume 3, Issue 1, July 2013

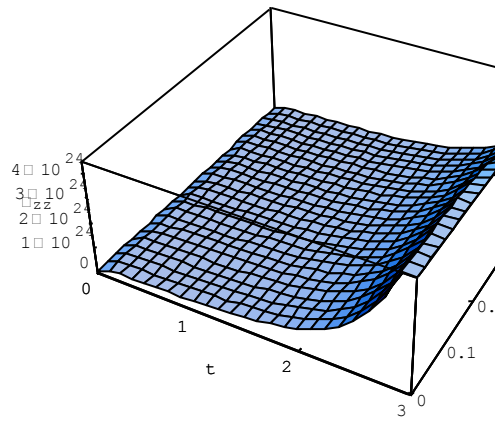

Fig. 12: Axial stress distribution along *r*-direction with varying time for z = 1.

$$\sigma_{rz} = 2G\left(\frac{1+\nu}{1-\nu}\right)\frac{a_t}{2a^2}\sum_{m,n=1}^{\infty}\frac{\cosh(\beta_n z)}{[J_0'(a\xi_n)]^2}\; e^{-kp^2 t}$$
$$\times[B(m)e^{-(\omega-kp^2)t} + 2kp^2\int \bar{\chi}^* e^{kp^2 t}dt + \bar{f}^*]$$
$$\times\left\{\frac{P_m'(z)}{\lambda_m\cosh(\beta_n z)}[r^2 J_0'(r\xi_n) + 2rJ_0(r\xi_n)]\right.$$
$$+(1-\nu)r^2 J_0(r\xi_n)[A_n J_1''(\beta_n r) + C_n(\beta_n r)J_1'''(\beta_n r)] + 3C_n\beta_n J_1''(\beta_n r)]$$
$$+(1-\nu)r[3rJ_0'(r\xi_n) + 7J_0(r\xi_n)]$$
$$\times[A_n J_0'(\beta_n r) + C_n(\beta_n r)J_1'(\beta_n r)] + C_n\beta_n J_1'(\beta_n r)]$$
$$+[(1-\nu)3r^2 J_0''(r\xi_n) + 14r(1-\nu)J_0'(r\xi_n) + (9-9\nu-\nu\beta_n^2 r^2)J_0(r\xi_n)]$$
$$\times[A_n J_0'(\beta_n r) + C_n(\beta_n r)J_1'(\beta_n r) + C_n\beta_n J_1(\beta_n r)]$$
$$+[(1-\nu)r^2 J_0'''(r\xi_n) + 7r(1-\nu)J_0''(r\xi_n) + (9-9\nu-\nu\beta_n^2 r^2)]$$
$$\times J_0'(r\xi_n) - 2\nu r\beta_n^2 J_0(r\xi_n)]$$
$$\left.\times[A_n J_0(\beta_n r) + C_n(\beta_n r)J_1(\beta_n r)]\right\} \qquad (30)$$

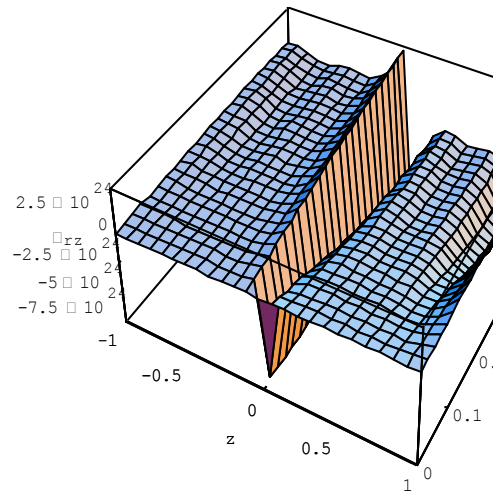

Fig. 13: Shear stress distribution along *r*- and *z*- direction for *t* =3

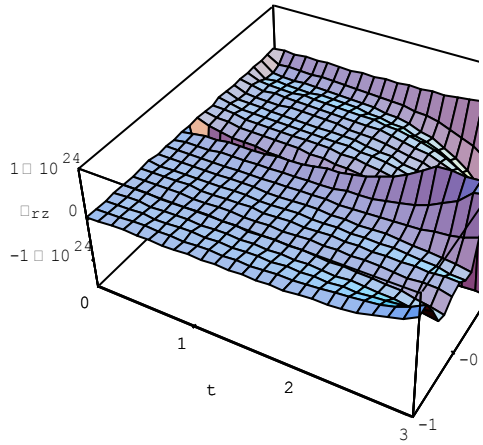

Fig. 14: Shear stress distribution along *z*-direction with varying time for r = 0.5

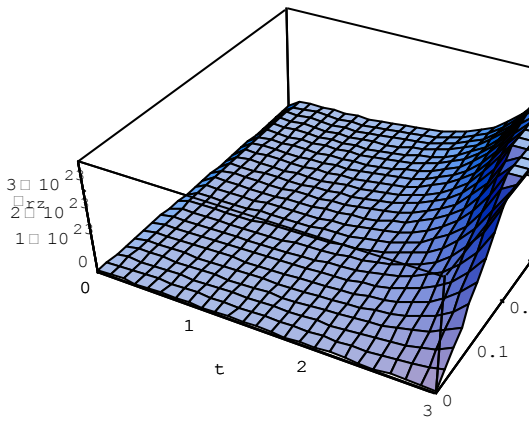

Fig. 15: Shear stress distribution along *r*-direction with varying time for z = 1.

Fig. 13 and 14 shows the Shear stress distribution σ_{rz} along the r and z direction of the solid cylinder at t = 3 and z-direction with varying time. A steep change in stress was found may be due to width of the plate. Shear stress also follows more sine waveform with high pecks and troughs along the z direction. Fig. 15 shows the Shear stress distribution along the radial direction of the plate with varying time. It is observed that stress gradually increases with time and is highest at the outer edge.

IV. SPECIAL CASE

Set $f(r,z) = z^2(a^2 - r^2)$ (31)

We first apply Hankel transform to equation (31) and then apply Marchi-Fasulo transform to get

$$\bar{f}^* = \frac{4aQ_n}{\beta_n^2 a_n^3}\left[\frac{2}{\beta_n}J_1(\beta_n a) - aJ_0(\beta_n a)\right]$$
$$\times[(a_n^2 h^2 - 2)\sin(a_n h) + 2a_n h\cos(a_n h)] \qquad (32)$$

Using equation (32) into equation (21) one obtains the expression for temperature distribution as

ISSN: 2277-3754
ISO 9001:2008 Certified
International Journal of Engineering and Innovative Technology (IJEIT)
Volume 3, Issue 1, July 2013

$$T=\frac{2}{a^2}\sum_{m,n=1}^{\infty}\frac{J_0(r\xi_n)}{[J_0'(a\xi_n)]^2}\frac{P_m(z)}{\lambda_m}e^{-kp^2t}$$

$$\times[B(m)e^{-(\omega-kp^2)t}+2kp^2\int\bar{\chi}^*e^{kp^2t}dt+\frac{4aQ_n}{\beta_n^2a_n^3}$$

$$\times\left[\frac{2}{\beta_n}J_1(\beta_n a)-aJ_0(\beta_n a)\right]$$

$$\times[(a_n^2h^2-2)\sin(a_nh)+2a_nh\cos(a_nh)] \quad (33)$$

V. NUMERICAL RESULTS, DISCUSSION AND REMARKS

Set $k_1=k_2=0.86$, r_0 = 0.20, z_0 = 0.5 and $\omega=0.5$ in equations (22) to (30).

Table 1: Material properties and parameters used in this study

Modulus of Elasticity, E	6.9×10^{11}
Shear modulus, G	2.7×10^{11}
Poisson ratio, υ	0.281
Thermal expansion coefficient α_t	25.5×10^{-6}
Thermal diffusivity, κ	0.86
Length, h	1 cm
Outer radius, b	0.5 m

VI. CONCLUSION

In this paper, the temperature distributions, displacement and stress functions of a circular plate in which sources are generated according to the linear function of the temperature have been obtained where the plate is subjected to known heat source function $\exp(-\omega t)\delta(r-r_0)$. As a particular case mathematical model is constructed for $f(r,z)=z^2(a^2-r^2)$ and performed numerical calculations. We develop the analysis for the temperature field by introducing the transformation techniques. Assigning suitable values to the parameters and functions in the equations of temperature, displacements and stresses respectively, expressions of special interest can be derived for any particular case of special interest.

ACKNOWLEDGEMENT

The authors are thankful to University Grant Commission, New Delhi for providing the partial financial assistance under major research project scheme.

REFERENCES

[1] Ishihara, Noda, Tanigawa: Journal of Thermal Stresses, Vol. 20; (1997), pp. 203-233.

[2] V.S. Kulkarni and K. C Deshmukh: Far East Journal of Applied Mathematics, Vol. 5, (2001), p.317- 329.

[3] N. W. Khobragade, D. B. Kamdi, and M. H Durge,: Int. Journal of Pure and Applied Maths, vol. 54, No. 3, (2009), p.387-406.

[4] E. Marchi and G Zgrablich. : Proc. Sindurdurgh Math. Soc. Vol. 14, part 2, (1964), pp.159-164.

[5] W. Nowacki,: Bull. Acad. Polon. Sci., ser. Sci., Tech., Vol. IV, No.5, 1957.

[6] S. K. Roychoudhary: Bull. Acad. Polon. Sci., Ser, Sci., Tech. No. 1, (1972), p.20-21.

[7] M. EI. Maghraby Nasser.: "Fourier Transforms", McGraw – Hill book company Inc, Chap.3; P.83, 1951.

[8] P. C. Wankhede: Indian J. of Pure and Applied Math. 13(11), (1982), pp. 1273-1277.

AUTHOR BIOGRAPHY

Dr. N.W. Khobragade For being M.Sc in statistics and Maths he attained Ph.D. He has been teaching since 1986 for 27 years at PGTD of Maths, RTM Nagpur University, Nagpur and successfully handled different capacities. At present he is working as Professor. Achieved excellent experiences in Research for 15 years in the area of Boundary value problems and its application. Published more than180 research papers in reputed journals. Fourteen students awarded Ph.D Degree and four students submitted their thesis in University for award of Ph.D Degree under their guidance.